IEEE Access
Multidisciplinary : Rapid Review : Open Access Journal

Received April 3, 2018, accepted May 14, 2018, date of publication June 18, 2018, date of current version June 29, 2018.

*Digital Object Identifier 10.1109/ACCESS.2018.2838328*

# Printed Quasi-Yagi Antennas Using Double Dipoles and Stub-Loaded Technique for Multi-Band and Broadband Applications

**KAI DA XU[1,2], (Member, IEEE), DAOTONG LI[3], (Member, IEEE), YANHUI LIU[1], (Member, IEEE), AND QING HUO LIU[4], (Fellow, IEEE)**
[1]Department of Electronic Science, Xiamen University, Xiamen 361005, China
[2]State Key Laboratory of Millimeter Waves, Southeast University, Nanjing 210096, China
[3]Center of Aerocraft TT&C and Communication, Chongqing University, Chongqing 400044, China
[4]Department of Electrical and Computer Engineering, Duke University, Durham, NC 27708 USA

Corresponding author: Daotong Li (dli@cqu.edu.cn)

This work was supported in part by the Venture and Innovation Support Program for Chongqing Overseas Returnees under Grant cx2017095, in part by the Fundamental Research Funds for the Central Universities under Grant 106112017CDJXY500002, in part by the National Natural Science Foundation of China under Grant 61601390, and in part by the State Key Laboratory of Millimeter Waves Open Research Program under Grant K201813.

**ABSTRACT** Double dipoles on a single-layer substrate are utilized to construct a triple-mode printed quasi-Yagi antenna for the multi-band and broadband antenna applications. A stub-loaded dipole generating two resonant modes (i.e., lower dual-mode dipole) is allocated on the underside of a simple dipole (i.e., upper single-mode dipole) introducing the third resonant mode. Using these three resonant modes, three compact printed quasi-Yagi antennas, i.e., tri-band, dual-band, and broadband printed quasi-Yagi antennas, are designed with the same antenna prototype but different parameter values. Seen from the measured results, all of these three antennas have good unidirectional radiations, high radiation efficiencies, and low cross-polarization levels at the operating frequencies within the impedance bandwidths.

**INDEX TERMS** Broadband antenna, dual-band antenna, quasi-Yagi antenna, stub-loaded technique, tri-band antenna.

## I. INTRODUCTION

Since the printed quasi-Yagi antenna on the dielectric substrate was first presented in [1], it has been researched extensively [2]–[6] due to its advantages of low profile, light weight and easy fabrication. For the antenna design of wireless communication systems, it is challenging to miniaturize antenna size while promoting its performance, such as low cost, high gain, wide impedance bandwidth and multiple operation bands. One of the most concerns is focused on the broadband printed quasi-Yagi antennas [7]–[10] or their operating bandwidth enhancement methods [11]–[13]. In [7] and [8], a coplanar waveguide and a coplanar stripline fed quasi-Yagi antennas are presented with the bandwidths of 44% and 41%, respectively. In order to further improve the bandwidths of the Yagi antennas, some researchers attempt to change the shapes of the drivers [9]–[11], reflectors [12] or directors [13].

In addition to the growing demand of the broadband antennas, the designs of multi-band antennas are also applied extensively to accomplish the requirements of multi-band and multi-service communication systems. Several dual-band printed Yagi antennas operating at two different frequency bands have been reported in [14]–[18]. For instance, in [17], the strip director of the printed Yagi antenna is replaced by two split ring resonators with two resonant modes for dual-band applications. In [18], a compact dual-band end-fire Yagi antenna is presented, where the roles of the driven dipole and director operating at the first frequency band are changed into the reflector and driven dipole at the second frequency band, respectively. Moreover, some tri-band printed quasi-Yagi antennas are proposed to meet the increasingly rapid-progress requirement of wireless communication systems [19]–[22]. In [19], a tri-band quasi-Yagi antenna with coplanar-waveguide-to-coplanar-strip transition is proposed, where the even-mode E-field at the coplanar-waveguide feed line can be smoothly transformed to the odd-mode E-field at the coplanar-strip line. Based on the conventional quasi-Yagi antennas, in [20]–[22], the additional operating modes are


2169-3536 © 2018 IEEE. Translations and content mining are permitted for academic research only.
Personal use is also permitted, but republication/redistribution requires IEEE permission.
See http://www.ieee.org/publications_standards/publications/rights/index.html for more information.

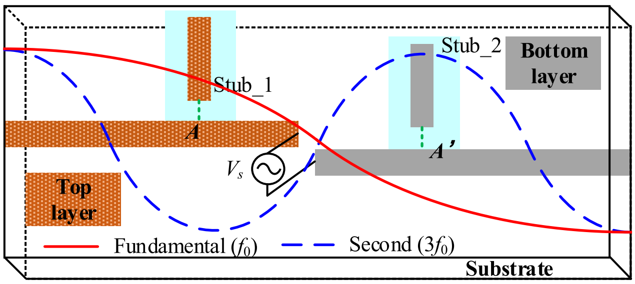


**FIGURE 1.** Geometry of the dual-mode stub-loaded dipole and voltage distributions of two resonant modes.

introduced by the changes of the drivers, reflectors or directors to obtain three desired frequency bands.

Stub-loaded technique is one of the most popular methods to generate an additional resonant mode in the design of microwave circuits and antennas [23], [24]. For instance, a stub-loaded slotline antenna is presented with two resonances in [25] and [26]. In this paper, double dipoles are employed with this stub-loaded technique for the triple-mode printed quasi-Yagi antenna applications. Two resonant modes are introduced by a stub-loaded dipole, named as the lower dual-mode dipole, and the third resonant mode is generated by a simple dipole, named as the upper single-mode dipole. The lower dual-mode dipole is allocated on the underside of the upper single-mode dipole. Finally, the miniaturized dual-band, tri-band, and broadband printed quasi-Yagi antennas using these two dipoles are designed, respectively.

## II. ANTENNA STRUCTURE AND ANALYSIS

Fig. 1 shows the geometry of the proposed stub-loaded dipole whose two arms are positioned on the top and bottom metallic layers of substrate, respectively. Based on a conventional dipole, two stubs are loaded at the trisection points ($A$ and $A'$) of the dipole. The voltage distributions of the first two operating modes are also plotted in Fig. 1, where the red solid line is the voltage distribution of the fundamental resonant mode at the frequency $f$, and the blue dash line represents the voltage distribution of the second resonant mode whose operating frequency is $3f0$. It can be seen that the voltage is maximum at the points $A$ and $A'$ for the second resonant mode, thus the two open stubs will affect this resonant mode but they have almost no effect on the fundamental resonant mode.

Fig. 2 shows the evolution of the triple-mode printed quasi-Yagi antenna. In Fig. 2(a), a conventional printed quasi-Yagi antenna is presented, which consists of a driven dipole and two short strips on the top and bottom metallic layers of the dielectric substrate as the director. The stepped impedance section in the input feedline is adopted for improving the impedance matching of the antenna. Then, a pair of strip lines are added to connect the driven dipole and the director as shown in Fig. 2(b), resulting in dual-mode generation. This is because that the previous director can behave as the driven dipole of the high-frequency mode while the previous driven

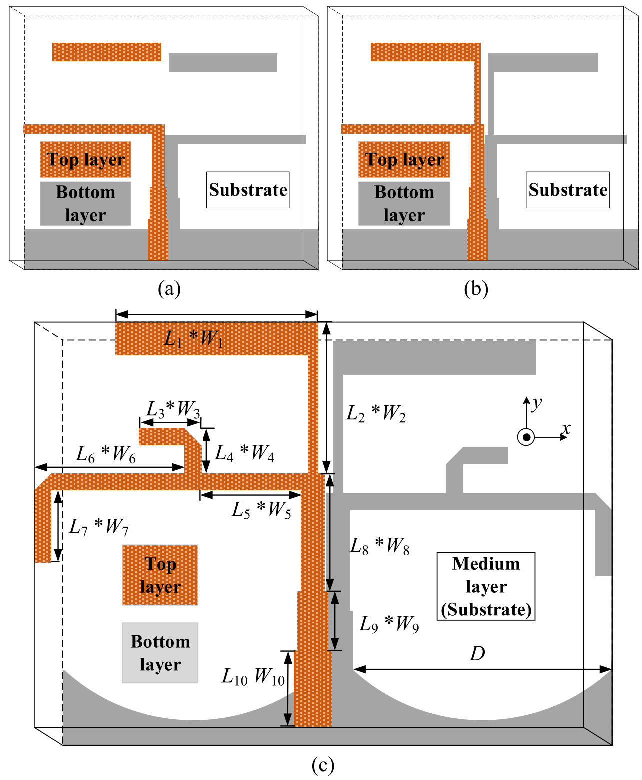


**FIGURE 2.** The evolution of the proposed triple-mode printed quasi-Yagi antenna. (a) Conventional printed quasi-Yagi antenna, (b) dual-mode printed quasi-Yagi antenna, and (c) the proposed triple-mode printed quasi-Yagi antenna with double concave parabolic reflector Substrate: FR4 with the relative dielectric constant of 4.4 and thickness of 1 mm.

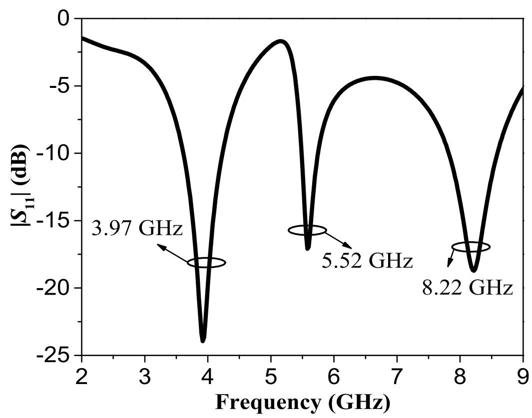


**FIGURE 3.** Simulated reflection coefficient of the tri-band printed quasi-Yagi antenna.

dipole behaves as the reflector. Finally, the third resonant mode is introduced by employing the stub-loaded technique as seen in Fig. 2(c). Two resonant modes are introduced by a stub-loaded dipole, named as the lower dual-mode dipole, whereas the third resonant mode is generated by a simple dipole, named as the upper single-mode dipole of the high-frequency mode. The lower dual-mode dipole and stubs are bended to minimize the occupied area of the antenna and keep from the touch of the upper single-mode dipole,

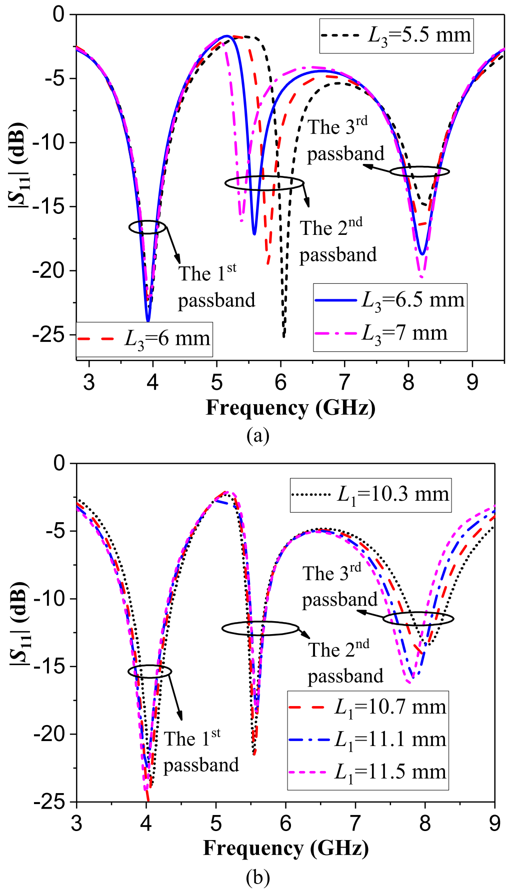


**FIGURE 4.** Simulated reflection coefficients of the tri-band printed quasi-Yagi antenna against the varied (a) $L_3$, and (b) $L_1$.

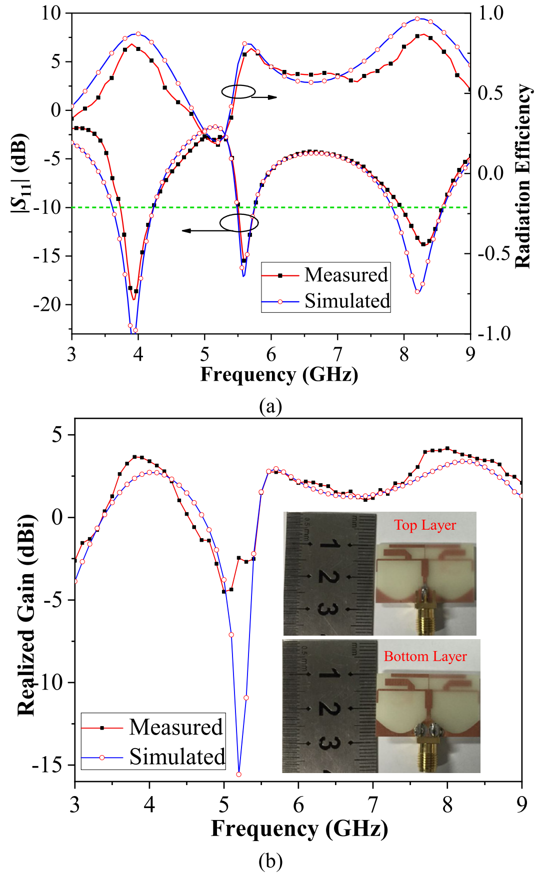


**FIGURE 5.** Simulated and measured (a) reflection coefficients and radiation efficiencies, and (b) realized gains at the end-fire direction of the proposed tri-band antenna. The fabricated photograph is shown in the inset.

respectively. Moreover, in order to increase the effective size of the ground plane, the symmetrical concave parabolic shape as the reflector is designed. By adjusting the positions of these above-mentioned three resonant modes, the printed quasi-Yagi antennas for dual-band, tri-band and broadband applications can be obtained.

## III. MULTI-BAND PRINTED QUASI-YAGI ANTENNAS

### A. TRI-BAND PRINTED QUASI-YAGI ANTENNA

For the design of a tri-band printed quasi-Yagi antenna, its antenna prototype is shown in Fig. 2(c), whose dimensions are set as follows (unit: mm): $W_1 = 1$, $W_2 = 0.1$, $W_3 = W_4 = 2$, $W_5 = W_6 = W_7 = 0.5$, $W_8 = 2$, $W_9 = 1$, $W_{10} = 1.85$, $L_1 = 10.9$, $L_2 = 4.5$, $L_3 = 8.5$, $L_4 = 1$, $L_5 = 3$, $L_6 = 8.85$, $L_7 = 3.5$, $L_8 = 5.4$, $L_9 = 3.2$, $W_{10} = 5$, and $D = 13.9$. The overall size of the antenna is 29.1 mm × 18.1 mm × 1 mm. Fig. 3 shows the reflection coefficient of the proposed tri-band printed quasi-Yagi antenna. The center frequency of the 1st passband is mainly determined by the overall length of the lower dual-mode dipole, i.e., $2(L_5 + L_6 + L_7)$, which can be adjusted to satisfy the required operating frequency. Then, the operating frequencies of the 2nd and 3rd passbands can be controlled independently. In Fig. 4(a), the center frequency of the 2nd passband can be adjusted by tuning the length of the $L_3$, while the center frequencies of the 1st and 3rd passbands keep fixed. This result agrees with the above-mentioned theoretical analysis in Section II. On the other hand, when the length of $L_1$ is changed, the center frequency of the 3rd passband will be shifted, but the center frequencies of the 1st and 2nd passbands have almost no change as shown in Fig. 4(b).

For demonstration, the tri-band printed quasi-Yagi antenna is fabricated, and a 50 Ω SMA connector is used to feed the antenna for measurement. As shown in Fig. 5(a), the three measured impedance bandwidths defined by $|S_{11}| < -10$ dB are 3.63423, 5.49-5.75 and 7.94-8.59 GHz, respectively, which are in good agreement with the simulations. The radiation efficiencies at the frequency range of 3-9 GHz are also measured, coincident with the simulated results. Fig. 5(b) illustrates the realized gains at the end-fire direction. Within the operating frequency ranging from 3.63 to 4.23 GHz, the simulated gain varies between 2 and 2.65 dBi, while the measured antenna gain varies between 2.6 and 4.67 dBi. For the 2nd passband of 5.495.75 GHz, the simulated gain varies between 1.8 and 2.91 dBi, and the measured counterpart ranges from 1.8 to 2.83 dBi. The simulated and measured gain variations in the 3rd passband of 7.94-8.59 GHz are

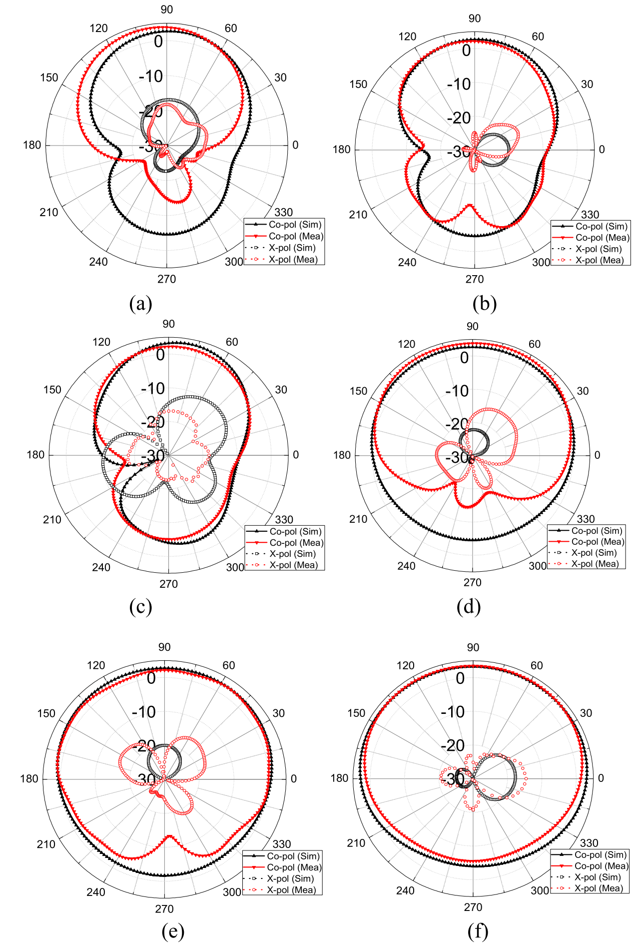


**FIGURE 6.** **Simulated and measured radiation patterns of the proposed tri-band antenna in E-plane at (a) 4 GHz, (b) 5.6 GHz, (c) 8.2 GHz and in H-plane at (d) 4 GHz, (e) 5.6 GHz, (f) 8.2 GHz.**

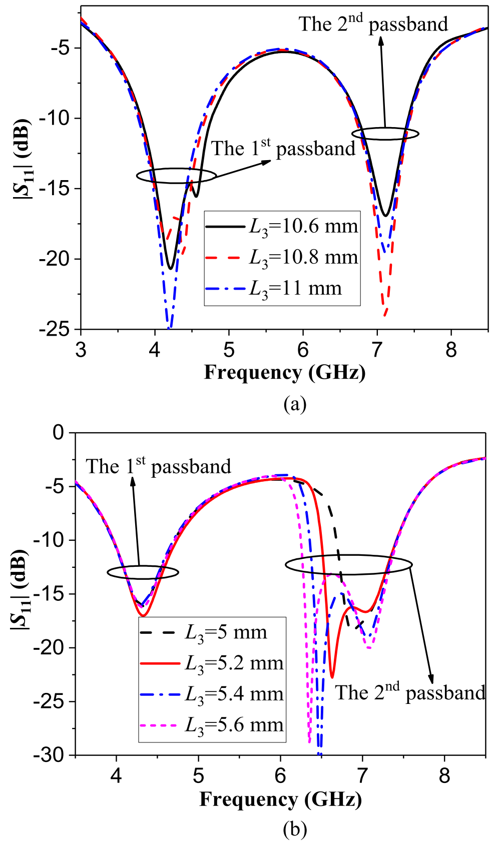


**FIGURE 7.** **Simulated reflection coefficients of the proposed dual-band quasi-Yagi antenna (a) under the first situation and (b) under the second situation against the varied $L_3$, where other parameters are set as $W_1 = 2$ mm$W_2 = 0.2$ mm, $W_3 = W_4 = 0.8$ mm, $W_5 = W_6 = W_7 = 1.1$ mm, $W_8 = 1.7$ mm, $W_9 = 1$ mm, $W_{10} = 1.85$ mm, $L_1 = 10.9$ mm, $L_2 = 6$ mm, $L_4 = 1$ mm, $L_5 = 4.5$ mm, $L_6 = 8$ mm, $L_7 = 2.9$ mm, $L_8 = 6.1$ mm, $L_9 = 3.2$ mm, $W_{10} = 5$ mm, $D = 13.2$ mm.**

2.93.31 dBi and 3.5-4.19 dBi, respectively The photograph of the fabricated antenna is shown in the inset of Fig. 5(b)

For indicating the radiation performance of the fabricated tri-band quasi-Yagi antenna, its radiation patterns at different frequencies are also measured. The comparisons of simulated and measured radiation patterns in E-plane (xoy-plane) and H-plane (yoz-plane) at 4 5.6, and 8.2 GHz are plotted in Fig. 6 The measured co-polarizations agree well with the simulated ones. The antenna achieves a front-to-back ratio (FBR) of over 18, 15 and 9 dB at 4 5.6 and 8.2 GHz, respectively. It can be observed that the proposed tri-band antenna has good unidirectional radiations with the main lobe in the *y*-axis direction, and low cross-polarization levels in both E- and H-planes at three different frequencies.

### *B. DUAL-BAND PRINTED QUASI-YAGI ANTENNA*

From Fig. 4(a), it can be seen that the second resonant mode can be shifted close to the first or third resonant mode, making two resonant modes adjacent each other. When we change the parameters of antenna prototype in Fig. 2(c) a dual-band printed quasi-Yagi antenna can be realized by using the three resonant modes, where two of them are employed to form one passband, and the remaining one constitutes the other passband. The bandwidths of these two passbands can be adjusted flexibly.

Fig. 7 illustrates the reflection coefficients of the proposed dual-band quasi-Yagi antennas under two situations. As seen from Fig. 7(a), the first two resonant modes are combined to form the 1st passband, and the third resonant mode consists of the 2nd passband. Meanwhile, the bandwidth of the 1st passband can be adjusted by tuning the length of $L_3$, but the 2nd passband has no change. For the second situation, the dual-band quasi-Yagi antenna can also be developed with a wider bandwidth of the 2nd passband as shown in Fig. 7(b). When the length of $L_3$ becomes shorter, the operating frequency of the second resonant mode will be shifted to the higher frequency, while the first and third resonant modes are fixed. Thus, the 2nd passband is achieved by the second and third resonant modes, and the 1st passband is realized by the first resonant mode. From Fig. 7(b), it can be also seen that the bandwidth of the 2nd passband can be adjusted by altering the length of $L_3$ while it is fixed for the first passband.

For demonstration, a printed quasi-Yagi antenna with dual-band response is fabricated and measured, whose dimensions in Fig. 2(c) are set as follows: $W_1 = 2$ mm, $W_2 = 0.2$ mm,

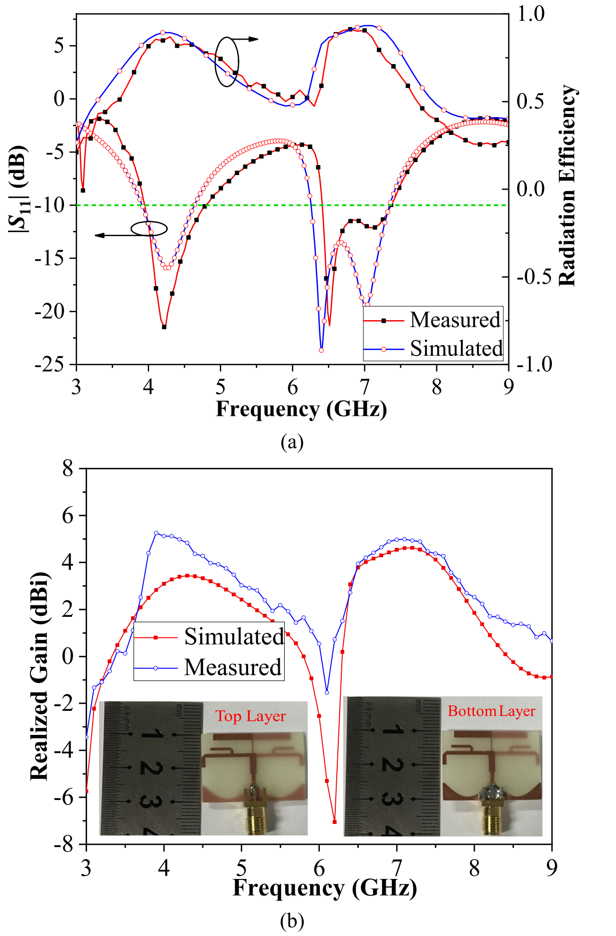


**FIGURE 8.** Simulated and measured (a) reflection coefficients and radiation efficiencies, and (b) realized gains at the end-fire direction of the proposed dual-band antenna. The fabricated photograph is shown in the inset.

$W_3 = W_4 = 0.8$ mm, $W_5 = W_6 = W_7 = 1.1$ mm, $W_8 = 1.7$ mm, $W_9 = 1$ mm, $W_{10} = 1.85$ mm, $L_1 = 10.9$ mm, $L_2 = 6$ mm, $L_3 = 6.3$ mm, $L_4 = 1$ mm, $L_5 = 4.5$ mm, $L_6 = 8$ mm, $L_7 = 2.9$ mm, $L_8 = 6.1$ mm, $L_9 = 3.2$ mm, $W_{10} = 5$ mm, $D = 13.2$ mm. The overall size of the antenna is 28.3 mm×20.3 mm×1 mm As shown in Fig. 8(a), the two measured impedance bandwidths with $|S_{11}| < -10$ dB are from 3.95 to 4.8 GHz and from 6.35 to 7.35 GHz, respectively, which are in agreement with the simulated ones. The radiation efficiencies within these two passbands are better than 70% and 75%, respectively. Fig. 8(b) illustrates the simulated and measured realized gains of the proposed dual-band antenna at the end-fire direction Within the two passbands of 3.95-4.8 GHz and 6.35-7.35 GHz, the measured gains at the end-fire direction are larger than 4 dBi and 3.8 dBi respectively The minor differences between simulations and measurements may be attributed to connector soldering and fabrication tolerances. The photograph of the fabricated dual-band antenna can be seen in the inset of Fig. 8(b).

The simulated and measured radiation patterns of the proposed dual-band antenna in E- and H-planes at 4.2 and 7.1 GHz are illustrated in Fig. 9. The experimental measurements have good agreement with the simulations. It can be observed that the co-polarized radiation patterns have good unidirectional radiations, realizing the FBR of around 19 and 13 dB at 4.2 and 7.1 GHz, respectively. The cross-polarization levels in the main lobe direction of the E- and H-planes at 4.2 and 7.1 GHz are all less than -20 dB

Performance comparisons between our work and some recent reported dual-band/tri-band antennas are tabulated in Table 1 It can be seen that the proposed dual-band and tri-band printed quasi-Yagi antennas fulfill the designs with unidirectional radiations, reasonable bandwidths and very miniaturized sizes.

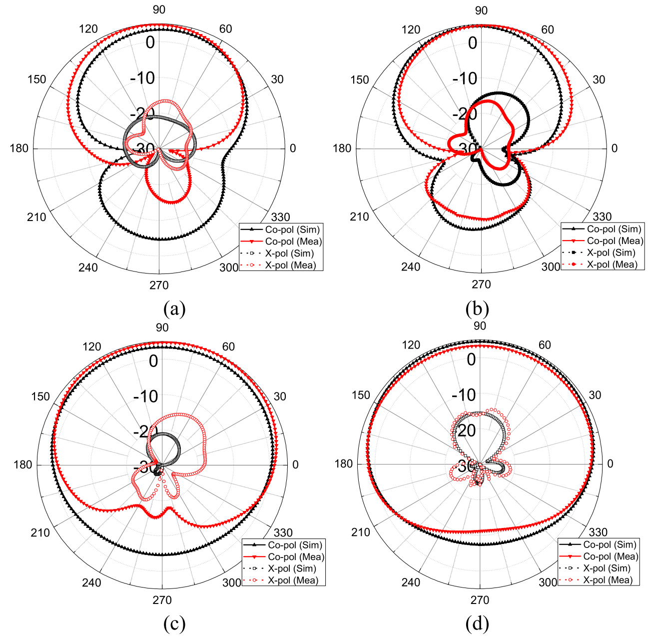


**FIGURE 9.** Simulated and measured radiation patterns of the proposed dual-band antenna in E-plane at (a) 4.2 GHz, (b) 7.1 GHz, and in H-plane at (c) 4.2 GHz, (d) 7.1 GHz.

**TABLE 1.** Comparisons of some recent multi-band printed Yagi antennas.

| Ref | Center Freq. (GHz) | Bandwidth (%) | Minimum FBR (dB) | Area ($\lambda_0 \times \lambda_0$) |
|---|---|---|---|---|
| [14] | 9.5 & 10.3 | 5.9 & 2 | ~19 | 1.84×0.92 (= 1.69) |
| [18] | 1.6 & 2.6 | 4 & 6.5 | 8 | 0.34×0.27 (= 0.09) |
| [20] | 0.82 & 1.7 & 2.4 | 29 & 20.9 & 2.2 | 7.3 | 0.3×0.22 (= 0.07) |
| [22] | 1.89 & 2.54 & 3.51 | 3.5 & 2.3 & 1.6 | 10.8 | 0.44×0.5 (= 0.22) |
| Prop. Dual-band Ant. | 4.38 & 6.85 | 19.4 & 14.6 | 13 | 0.37×0.26 (= 0.1) |
| Prop. Tri-band Ant. | 3.9 & 5.62 & 8.27 | 15.4 & 4.6 & 7.9 | 9 | 0.35×0.34 (= 0.12) |

## IV. BROADBAND PRINTED QUASI-YAGI ANTENNA

The proposed antenna prototype can also be designed into a broadband printed quasi-Yagi antenna through tuning the parameters shown in Fig. 2(c). For demonstration,

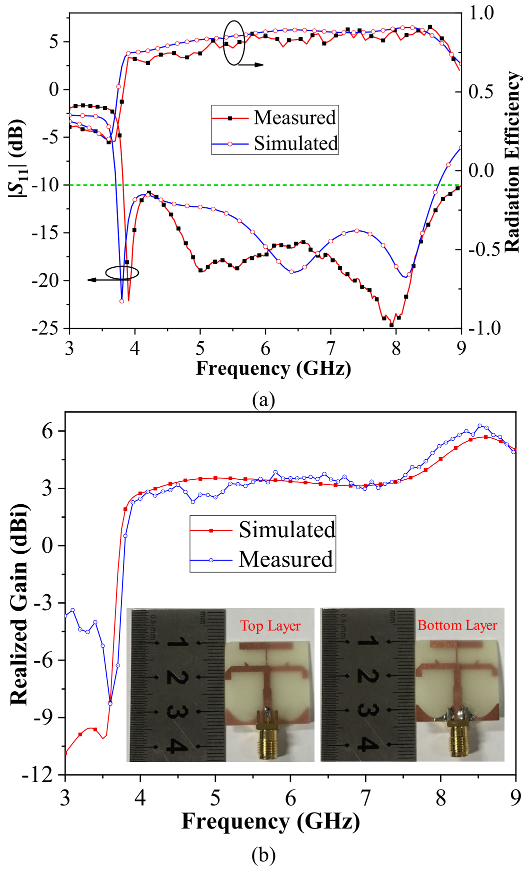


**FIGURE 10.** Simulated and measured (a) reflection coefficients and radiation efficiencies, and (b) realized gains at the end-fire direction of the proposed broadband antenna. The fabricated photograph is shown in the inset.

a broadband antenna is fabricated and measured, whose dimensions are as follows: $W_1 = 2.1$ mm, $W_2 = 0.3$ mm, $W_3 = W_4 = 1$ mm, $W_5 = W_6 = W_7 = 1.8$ mm, $W_8 = 1.7$ mm, $W_9 = 2.3$ mm, $W_{10} = 1.85$ mm, $L_1 = 7.9$ mm, $L_2 = 6.9$ mm, $L_3 = 1.2$ mm, $L_4 = 0.2$ mm, $L_5 = 4.3$ mm, $L_6 = 5.85$ mm, $L_7 = 2.2$ mm, $L_8 = 6.8$ mm, $L_9 = 5.4$ mm, $W_{10} = 5$ mm, $D = 10.85$ mm. The overall size of the antenna is 24 mm×24.1 mm×1 mm. As shown in Fig. 10(a), the simulated impedance bandwidth with $|S_{11}| < -10$ dB is from 3.71 to 8.65 GHz (80%) and the measured counterpart is from 3.8 to 9 GHz (81.3%). The measured radiation efficiencies within the passband are better than 72%, in good agreement with the simulated results Fig. 10(b) shows the simulated and measured gain variations of the broadband antenna with the frequency In the operating frequency band of 3.8-9 GHz, the measured gains at the end-fire direction vary from 2.7 to 6 dBi The fabricated photograph is embedded in the inset of Fig. 10(b).

For illustrating the radiation performance of the fabricated broadband quasi-Yagi antenna, its radiation patterns are measured at three different frequencies, i.e. 4.5, 6, and 7.5 GHz. The simulated and measured radiation patterns including co-polarizations and cross-polarizations in E- and H-planes, respectively, are plotted in Fig. 11, where stable radiation patterns can be obtained. It can be observed that the proposed broadband antenna has low cross-polarization levels in both E and H-planes, and high unidirectional radiations with the FBR of 15, 17 and 15 dB at 4.5, 6 and 7.5 GHz, respectively. Performance comparisons between our proposed broadband antenna and some other reported works are also tabulated in Table 2 As can be seen, our design has achieved wide bandwidth, high FBR and very compact size simultaneously.

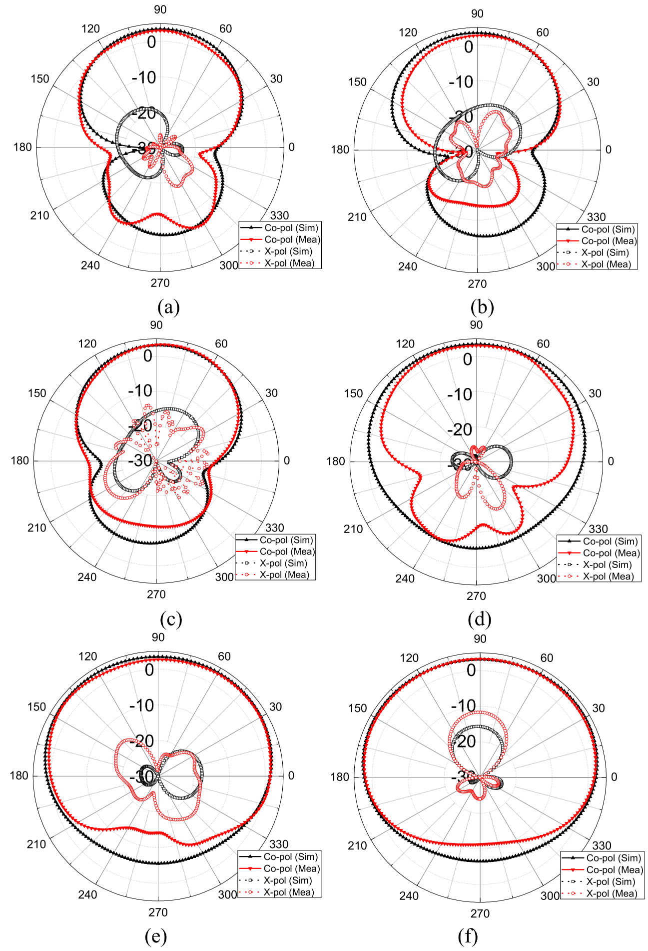


**FIGURE 11.** Simulated and measured radiation patterns of the proposed broadband antenna in E-plane at (a) 4.5 GHz, (b) 6 GHz, (c) 7.5 GHz and in H-plane at (d) 4.5 GHz, (e) 6 GHz, (f) 7.5 GHz.

**TABLE 2.** Comparisons of some recent broadband printed Yagi antennas.

| Ref | Center Freq. (GHz) | BW (%) | Min FBR (dB) | Area ($\lambda_0 \times \lambda_0$) |
|---|---|---|---|---|
| [4] | 2.4 | 8 | 15 | 0.5 × 0.45 = 0.23 |
| [5] | 0.9 | 48 | 8 | 0.28 × 0.23 = 0.06 |
| [6] | 2.4 | 8 | 15 | 0.46 × 0.38 = 0.17 |
| [12] | 7 | 100 | 10 | 0.36 × 0.41 = 0.15 |
| Prop. | 6.4 | 81.3 | 15 | 0.3×0.3 = 0.09 |

## V. CONCLUSION

Using the same antenna geometry and stub-loaded technique, three double-dipoles-based printed quasi-Yagi antennas have been designed for the tri-band, dual-band and broadband applications, respectively, in this paper. These three antennas have been fabricated on the low-cost FR4 substrate with very compact sizes. The measured results illustrate that all of the printed quasi-Yagi antennas have reasonable impedance bandwidths, good unidirectional radiations, high radiation efficiencies and low cross-polarization levels within the operating frequency bands

## REFERENCES


[1] J. Huang and A. C. Densmore, "Microstrip Yagi array antenna for mobile satellite vehicle application," *IEEE Trans. Antennas Propag.*, vol. 39, no. 7, pp. 1024–1030, Jul. 1991.

[2] W. R. Deal, N. Kaneda, J. Sor, Y. Qian, and T. Itoh, " A new quasi-Yagi antenna for planar active antenna arrays," *IEEE Trans. Microw. Theory Techn.*, vol. 48, no. 6, pp. 910–918, Jun. 2000.

[3] Y. Cai, Y. J. Guo, and A. R. Weily, " A frequency-reconfigurable quasi-Yagi dipole antenna," *IEEE Trans. Antennas Wireless Propag.*, vol. 58, pp. 883–886, 2010.

[4] R. Bhattacharya, R. Garg, and T. K. Bhattacharyya, "A compact Yagi–Uda type pattern diversity antenna driven by CPW-fed pseudomonopole," *IEEE Trans. Antennas Propag.*, vol. 64, no. 1, pp. 25–32, Jan. 2016.

[5] S. A. Rezaeieh, M. A. Antoniades, and A. M. Abbosh, "Miniaturized planar Yagi antenna utilizing capacitively coupled folded reflector," *IEEE Antennas Wireless Propag. Lett.*, vol. 16, pp. 1977–1980, 2017.

[6] Y. Luo and Q.-X. Chu, "A Yagi–Uda antenna with a stepped-width reflector shorter than the driven element," *IEEE Antennas Wireless Propag. Lett.*, vol. 15, pp. 564–567, 2016.

[7] H. K. Kan, R. B. Waterhouse, A. M. Abbosh, and M. E. Bialkowski, "Simple broadband planar CPW-fed quasi-Yagi antenna," *IEEE Antennas Wireless Propag. Lett.*, vol. 6, pp. 18–20, 2007.

[8] K. Han, Y. Park, H. Choo, and I. Park, "Broadband CPS-fed Yagi–Uda antenna," *Electron. Lett.*, vol. 45, no. 24, pp. 1207–1209, Nov. 2009.

[9] P. T. Nguyen, A. Abbosh, and S. Crozier, "Wideband quasi-Yagi antenna with tapered driver," in *Proc. IEEE Asia–Pacific Conf. Antennas Propag.*, Singapore, Aug. 2012, pp. 138–139.

[10] J. Wu, Z. Zhao, Z. Nie, and Q. H. Liu, "A broadband unidirectional antenna based on closely spaced loading method," *IEEE Trans. Antennas Propag.*, vol. 61, no. 1, pp. 109–116, Jan. 2013.

[11] J. Yeo and J.-I. Lee, "Bandwidth enhancement of double-dipole quasi-Yagi antenna using stepped slotline structure," *IEEE Antennas Wireless Propag. Lett.*, vol. 15, pp. 694–697, 2016.

[12] J. Wu, Z. Zhao, Z. Nie, and Q.-H. Liu, "Bandwidth enhancement of a planar printed quasi-Yagi antenna with size reduction," *IEEE Trans. Antennas Propag.*, vol. 62, no. 1, pp. 463–467, Jan. 2014.

[13] L. Lu, K. Ma, F. Meng, and K. S. Yeo, "Design of a 60-GHz quasi-Yagi antenna with novel ladder-like directors for gain and bandwidth enhancements," *IEEE Antennas Wireless Propag. Lett.*, vol. 15, pp. 682–685, 2016.

[14] X. S. Yang, B. Z. Wang, W. Wu, and S. Xiao, "Yagi patch antenna with dual-band and pattern reconfigurable characteristics," *IEEE Antennas Wireless Propag. Lett.*, vol. 6, pp. 168–171, 2007.

[15] S. Lim and M. F. Iskander, "Design of a dual-band, compact Yagi antenna over an EBG ground plane," *IEEE Antennas Wireless Propag. Lett.*, vol. 8, pp. 88–91, 2009.

[16] H. Sun, Y.-X. Guo, M. He, and Z. Zhong, "A dual-band rectenna using broadband Yagi antenna array for ambient RF power harvesting," *IEEE Antennas Wireless Propag. Lett.*, vol. 12, pp. 918–921, 2013.

[17] D. O. Kim and C. Y. Kim, "Dual-band quasi-Yagi antenna with split ring resonator directors," *Electron. Lett.*, vol. 48, no. 14, pp. 809–810, Jul. 2012.

[18] H. C. Huang, J. C. Lu, and P. Hsu, "A compact dual-band printed Yagi–Uda antenna for GNSS and CMMB applications," *IEEE Trans. Antennas Propag.*, vol. 63, no. 5, pp. 2342–2348, May 2015.

[19] Y. Ding, Y. C. Jiao, P. Fei, B. Li, and Q. T. Zhang, "Design of a multiband quasi-Yagi-type antenna with CPW-to-CPS transition," *IEEE Antennas Wireless Propag. Lett.*, vol. 10, pp. 1120–1123, 2011.

[20] S.-J. Wu, C.-H. Kang, K,-H. Chen, J.-H. Tarng, "A multiband quasi-Yagi type antenna," *IEEE Trans. Antennas Propag.*, vol. 58, no. 2, pp. 593–596, Feb. 2010.

[21] J. Yeo and J. I. Lee, "Design of tri-band double-dipole quasi-Yagi antenna using dual co-directional SRRs," *Microw. Opt. Technol. Lett.*, vol. 59, no. 6, pp. 1354–1357, 2017.

[22] P. Cheong, K. Wu, W.-W. Choi, and K.-W. Tam, "Yagi–Uda antenna for multiband radar applications," *IEEE Antennas Wireless Propag. Lett.*, vol. 13, pp. 1065–1068, 2014.

[23] X. Y. Zhang, J.-X. Chen, Q. Xue, and S.-M. Li, " Dual-band bandpass filters using stub-loaded resonators," *IEEE Microw. Wireless Compon. Lett.*, vol. 17, no. 8, pp. 583–585, Aug. 2007.

[24] W.-J. Lu, L. Zhu, K. W. Tam, and H.-B. Zhu, "Wideband dipole antenna using multi-mode resonance concept," *Int. J. Microw. Wireless Technol.*, vol. 9, no. 2, pp. 365–371, Mar. 2017.

[25] W. J. Lu and L. Zhu, "Wideband Stub-loaded slotline antennas under multi-mode resonance operation," *IEEE Trans. Antennas Propag.*, vol. 63, no. 2, pp. 818–823, Feb. 2015.

[26] W. J. Lu and L. Zhu, "A novel wideband slotline antenna with dual resonances: Principle and design approach," *IEEE Antennas Wireless Propag. Lett.*, vol. 14, pp. 795–798, 2015.


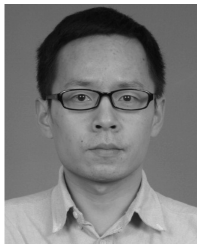

**KAI DA XU** (S'13–M'15) received the B.S. and Ph.D. degrees in electromagnetic field and microwave technology from the University of Electronic Science and Technology of China (UESTC), Chengdu, China, in 2009 and 2015, respectively. From 2012 to 2014, he was a Visiting Researcher with the Department of Electrical and Computer Engineering, Duke University, Durham, NC, USA, under the financial support from the China Scholarship Council. From 2016 to 2017, he was a Post-Doctoral Fellow with the State Key Laboratory of Millimeter Waves, City University of Hong Kong, Hong Kong. He is currently an Assistant Professor with the Institute of Electromagnetics and Acoustics and the Department of Electronic Science, Xiamen University, Xiamen, China. He has authored or co-authored over 80 papers in peer-reviewed journals and conference proceedings. His current research interests include RF/microwave and mm-wave circuits, antenna arrays, and nanoscale memristors. He was the recipient of the UESTC Outstanding Graduate Awards in 2009 and 2015, respectively. He was a recipient of the National Graduate Student Scholarship from the Ministry of Education, China, in 2012, 2013, and 2014. He is serving as a Reviewer for several IEEE and IET journals, including the IEEE Transactions on Microwave Theory and Techniques, the IEEE Transactions on Electron Devices, the IEEE Transactions on Computer-Aided Design of Integrated Circuits and Systems, *IEEE Microwave Magazine*, IEEE Antennas and Wireless Propagation Letters, IEEE Microwave and Wireless Components Letters, IEEE Access, *IET Microwaves Antennas & Propagation*, and *Electronics Letters*. Since 2017, he has been serving as an Associate Editor for IEEE Access and *Electronics Letters*. He is also an Editorial Board member of the *AEÜ-International Journal of Electronics and Communications*.

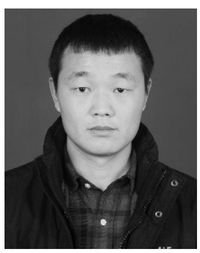

**DAOTONG LI** (S'15–M'16) received the Ph.D. degree in electromagnetic field and microwave technology from the University of Electronic Science and Technology of China (UESTC), Chengdu, China, in 2016. Since 2015, he has been a Visiting Researcher with the Department of Electrical and Computer Engineering, University of Illinois at Urbana–Champaign, Urbana, IL, USA, with the financial support from the China Scholarship Council. He is currently with the Center of Aircraft TT&C and Communication, Chongqing University, Chongqing. He has authored or co-authored over 30 peer-reviewed journal or conference papers. Since 2014, he has been a Reviewer for some international journals. His current research interests include RF, microwave and millimeter-wave technology and applications, antennas, devices, circuits and systems, and passive and active (sub-) millimeter-wave imaging, and radiometer. He was a recipient of the UESTC Outstanding Graduate Awards by the Sichuan province and UESTC in 2016. He was also a recipient of the National Graduate Student Scholarship from the Ministry of Education, China, and the Tang Lixin Scholarship.

**YANHUI LIU** (M'15) received the B.S. and Ph.D. degrees in electrical engineering from the University of Electronic Science and Technology of China (UESTC), Chengdu, China, in 2004 and 2009, respectively. From 2007 to 2009, he was a Visiting Scholar with the Department of Electrical Engineering, Duke University, Durham, NC, USA. Since 2011, he has been with Xiamen University, China, where he is currently a Full Professor with the Department of Electronic Science. In 2017, he was a Visiting Professor with the State Key Laboratory of Millimeter Waves, City University of Hong Kong. He has authored or co-authored over 110 peer-reviewed journal and conference papers. He holds several granted Chinese patents. His research interests include antenna array design, array signal processing, and microwave imaging methods. He was the recipient of the UESTC Outstanding Graduate Award in 2004 and the Excellent Doctoral Dissertation Award of Sichuan Province of China in 2012. He is serving as a Reviewer for several international journals, including the IEEE Transactions on Antennas and Propagation, the IEEE Transactions on Geosciences and Remote Sensing, IEEE Antennas and Wireless Propagation Letters, IEEE Microwave and Wireless Components Letters, *IET Microwave, Antennas and Propagation*, and *Digital Signal Processing*. Since 2018, he has been serving as an Associate Editor for IEEE Access.

**QING HUO LIU** (S'88–M'89–SM'94–F'05) received the B.S. and M.S. degrees in physics from Xiamen University, China, and the Ph.D. degree in electrical engineering from the University of Illinois at Urbana–Champaign. He was with the Electromagnetics Laboratory, University of Illinois at Urbana–Champaign, as a Research Assistant from 1986 to 1988, and as a Post-Doctoral Research Associate from 1989 to 1990. He was a Research Scientist and a Program Leader with Schlumberger-Doll Research, Ridgefield, CT, USA, from 1990 to 1995. From 1996 to 1999, he was an Associate Professor with New Mexico State University. Since 1999, he has been with Duke University, where he is currently a Professor of electrical and computer engineering. He has authored or co-authored over 400 papers in refereed journals and 500 papers in conference proceedings. His research interests include computational electromagnetics and acoustics, inverse problems, and their application in nanophotonics, geophysics, biomedical imaging, and electronic packaging. He is a Fellow of the Acoustical Society of America, the Electromagnetics Academy, and the Optical Society of America. He was the recipient of the 1996 Presidential Early Career Award for Scientists and Engineers from the White House, the 1996 Early Career Research Award from the Environmental Protection Agency, and the 1997 CAREER Award from the National Science Foundation. He was also the recipient of the ACES Technical Achievement Award in 2017. He currently serves as the Founding Editor-in-Chief of the IEEE Journal on Multiscale and Multiphysics Computational Techniques, the Deputy Editor-in-Chief of *Progress in Electromagnetics Research*, and an Editor of the *Journal of Computational Acoustics*. He served as an IEEE Antennas and Propagation Society Distinguished Lecturer for 2014-2016.